https://doi.org/10.18321/ectj1033

Advanced Characterization of Bituminous Binders: Comparing Industrial and Paving-Grade Bituminous Binders

S. Eskandarsefat[1]*, P. Caputo[2], C. Oliviero Rossi[2], R. Vaiana[2], C. Sangiorgi[1]

[1]DICAM-Roads, Department of Civil, Chemical, Environmental and Materials Engineering, University of Bologna, V.le Risorgimento 2, 40136, Bologna, Italy
[2]University of Calabria, Ponte P. Bucci, Arcavacata di Rende, 87036 Campus di Arcavacata di Rende (CS), Italy

Article info

Received:
5 June 2020

Received in revised form:
16 August 2020

Accepted:
24 October 2020

Keywords:
Industrial bitumen
Paving-grade bitumen
Chemical analysis
Thermal analysis
Rheological analysis

Abstract

This paper deals with the fundamental differences between industrial and paving-grade bituminous binders. The paper is presented in two main sections: 1) a review of the materials' colloidal structure and the required properties for the industrial and paving applications; 2) a wide range of experimental tests with which the bituminous binders were studied and compared. In this research, a 160/220 industrial bitumen was studied and compared to a paving-grade bitumen with the same penetration and with a lower penetration, 70/100 one. The research consisted of physical, chemical, thermal, microstructural, and rheological analysis to provide a comprehensive understanding of these bituminous binders of diverse applications. Overall, the comparison of the tests' results indicated that while the asphaltene content and its characteristics have a great influence on the bitumen's properties, it is not the only fundamental factor. During the study of the chemical structures via Atomic Force Microscopy (AFM), it was found that the Peri phase (attributed to the resins) also plays an important role, defining the bitumen's physical visco-elastic properties. In fact, from a microstructural point of view using AFM a significant difference was notified between the industrial bitumen and the paving-grade ones. These differences allow the paving-grade bitumens to be more elastic and ductile compared to the industrial bitumen.

1. Introduction

1.1. On the type of bituminous binding products

Frequently-used blackish, viscous, and sticky material: bitumen is known for its complex characteristics, which can often induce difficulties in its applications. Bitumen is manufactured from the distillation of crude oil during petroleum refining. It is produced to meet a variety of specifications based upon physical properties for specific end uses. Its main characteristics as an adhesive, as well as being waterproof, thermoplastic, durable, modifiable and recyclable making it ideal as a construction and engineering material. There are more than 250 known applications of bitumen, with the majority of bitumen being used in paving and roofing applications [1]. It is estimated that globally about 85% of all the bitumen to be used as a binder in various kinds of asphalt pavements, about 10% of global bitumen production to be used for roofing applications, and the remaining 5% is used for a variety of building materials such as pipe coatings, carpet backing, joint sealants, and paint [2]. Thus considering the main application, bitumen can be mainly divided into two groups of 1) paving-grade and 2) industrial bitumens, which includes also the roofing bitumens. In short, the term roofing bitumen is largely meaningless, and if used to denote the hot-applied products that characterized the industry decades ago, misleading and erroneous [3]. The many different types of bitumen used in current-day roofing exhibit dramatic differences in engineering properties. While the term roofing bitumen and oxidize bitumen are often used interchangeably in

*Corresponding author.
E-mail: shahin_esft@yahoo.com

literature and sometimes synonymous, an oxidized bitumen product is just one of the diverse types of bitumen-based products used in the roofing industry. Oxidized Bitumen or Blown bitumen grades are produced by passing air through the penetration grades [4]. This process gives the bitumen more rubbery properties than its original formula and they are simply harder bitumen. Oxidized Bitumen has a wide variety of industrial applications such as bonding bitumen for roofing membranes, hot-applied waterproofing layers, carpet tile manufacture, liquid bitumen coatings, the production of bituminous paint, mastic and etc.

Comparing the engineering specifications of the bituminous binders to be used in the fields of pavement construction and industrial applications, significant differences exist. Paving-grade bitumens are characterised by low-penetration and preferred more elastic properties. Given its adhesion and cohesion properties and high impermeability, paving bitumen offers resistance to most acids and salts, in this way it guarantees long-lasting performance; moreover, this material can be recycled [5]. These bitumens are nowadays classified based on penetration, viscosity, and performance depend on the specifications. In comparison, industrial bitumens except for those of oxidized ones are of low penetrations. For industrial applications e.g. production of bituminous membranes, electrical and thermal insulations, the properties of the bitumen must guarantee the resistance to aging and oxidation under various weather conditions, as well as protection, flexibility and impermeability [6]. From another perspective, considering the level of bitumen modification, there is also a significant difference between the modified paving-grade bitumens compared to the industrially-used ones. While for the modified paving-grade bitumens (here refers to the most common bitumen modification using SBS copolymers) the quantity of the polymer is usually less than 5% (by the weight of bitumen) and the bitumen provides the matrix of the compound, for the industrial bitumens, the polymer itself makes the matrix of the compound [7, 8]. For instance, due to the low cost and waste-based, polymeric products such as atactic polypropylene can be used in a quantity as high as 25% in some industrial applications. Specific chemical characteristics are designed to provide compatibility with polypropylene polymers, SBS compounds (elastomeric polymers) and polymers of self-adhesive elastomeric membranes [5, 9]. For instance, it has been shown that both the compatibility and stability of polymer-added bitumens depend not only on the difference in density and viscosity between bitumen and polymer but also on bitumen's microstructure and its chemical properties [10, 11], in which these bitumens are different.

1.2. Bitumen from a chemical perspective

From a chemical point of view, apart from the original properties of the crude oil and the processing technique, bitumen is a composite material that can be easily separated into two major fractions by solvent extraction with n-heptane. These fractions are the insoluble fraction of asphaltenes and the soluble fraction known as maltenes. Maltenes as soluble part in n-heptane can in turn, be subdivided into saturates, aromatics, and resins, which, together with the asphaltenes, are known as SARA fractions. It should be noted that the percentage of the fractions depends on the crude oil origin, the manufacturing process and the grade of the bitumen.

To date, several colloidal models have been introduced, describing the bitumen chemical structure, however as shown in Fig. 1 the bitumen's structure can be described as a colloidal dispersion of asphaltene micelles into maltene. According to the relative proportion of asphaltene and resins, shown in Table 1, three different types of colloidal structures, namely sol, gel, and sol-gel bitumen can be recognized [12]. In the sol-type bitumen the asphaltene micelles are fully dispersed without any interaction that leads to Newtonian behaviour. The sol-type bitumen is characterized by a greater fluidity, plasticity, and temperature sensitivity, but low viscosity [13] on the contrary, a gel bitumen contains a higher content of asphaltene and fully interconnected micelles showing a highly non-Newtonian behaviour. The gel-type asphalt is characterized by an inferior fluidity, plasticity, and temperature sensitivity, but a higher viscosity. Between these two extremes, the majority of bitumens were found to have an intermediate behaviour because of the mixed sol-gel structure. The bitumens of this structure are considered as paving-grade bitumens [14].

Table 1
Types of bitumen structure vs. composition [12]

Bitumen Type	Asphaltenes (%)	Resins (%)	Oils (%)
Sol bitumen	< 18	> 36	< 48
Gel bitumen	> 25	< 24	> 50
Sol-Gel bitumen	21 to 23	30 to 34	45 to 49

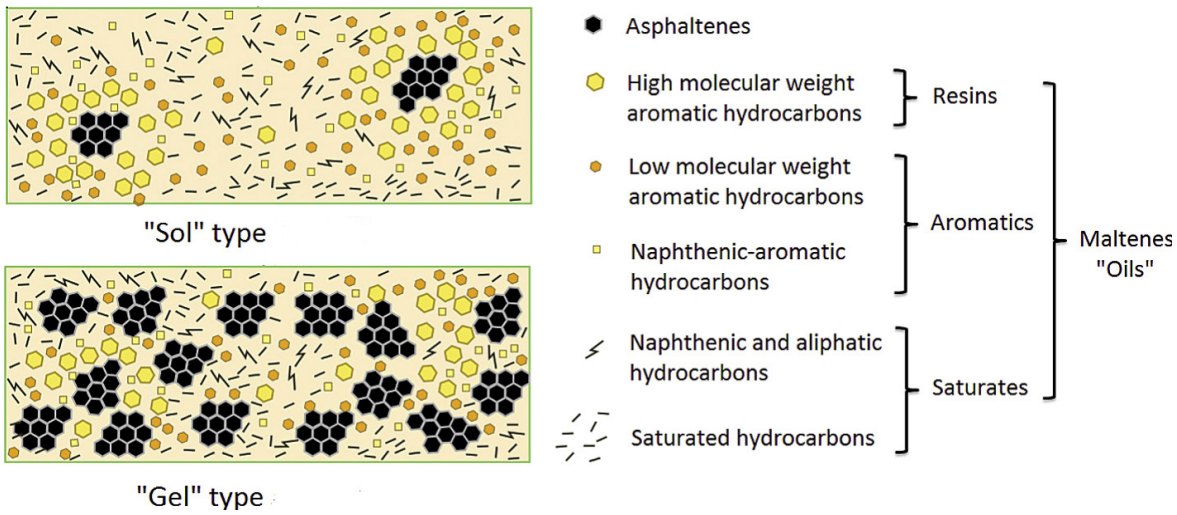

Fig. 1. Schematic model of bitumen's colloidal structure [10].

1.3. Problem statement and objectives

It has sometimes been assumed that once the chemistry of bitumen is known we will be able to predict its performance as a construction material, however, the knowledge of the chemical composition is also a limited help for understanding bitumen and some of the advanced analytical are not easily translated to physical properties. For this purpose, in continuation of the authors' former paper [15–17], aimed at an interdisciplinary study on the fundamental differences between paving-grade and industrially-used bitumens. The authors believe that the outcomes of this study could provide new insights into the characteristics of these two major categories of bitumens. However, the authors believe that for having universal deductions further research on bitumens of different origins is still needed to be carried out.

2. Materials

Considering the objectives of this research, three different penetration-graded bitumens were investigated: a 70/100 and a 160/220 paving-grade bitumen and a 160/220 industrial bitumen. Table 2 compares some of the physical properties of the bitumens. While generally the 160/220 paving-grade bitumen is primarily used for the production of bituminous emulsions, the 160/220 industrial bitumen has been designed for compounds with high polymer content such as waterproofing membranes and sealing materials. As mentioned before, the industrial bitumen has high compatibility with high polymer content modification while the same grade paving one has poor compatibility with high polymer proportion.

3. Methods

The experimental program of the presented research consisted of five sections, providing a comprehensive understanding of the characteristics of industrial and paving-grade bitumens. Figure 2 shows the research plan and applied testing methods.

Table 2
Some of the properties of the bitumens

Measured properties	Test method	Unit	Paving-grade		Industrial
			70/100	160/220	160/220
Penetration @25 °C	EN 1426	0.1 mm	70-100	160-220	160-220
Softening Point (R&B)	EN 1427	°C	46	41	39
Upper PG	AASHTO	°C	58	52	52
Flash Point	EN 2592	°C	≥ 230	≥ 220	≥ 220
Dynamic Viscosity @ 60 °C	EN 12596	Pa.s	≥ 90	≥ 30	-
Fraass Breaking Point	EN 12593	°C	≤ -10	≤ -15	-

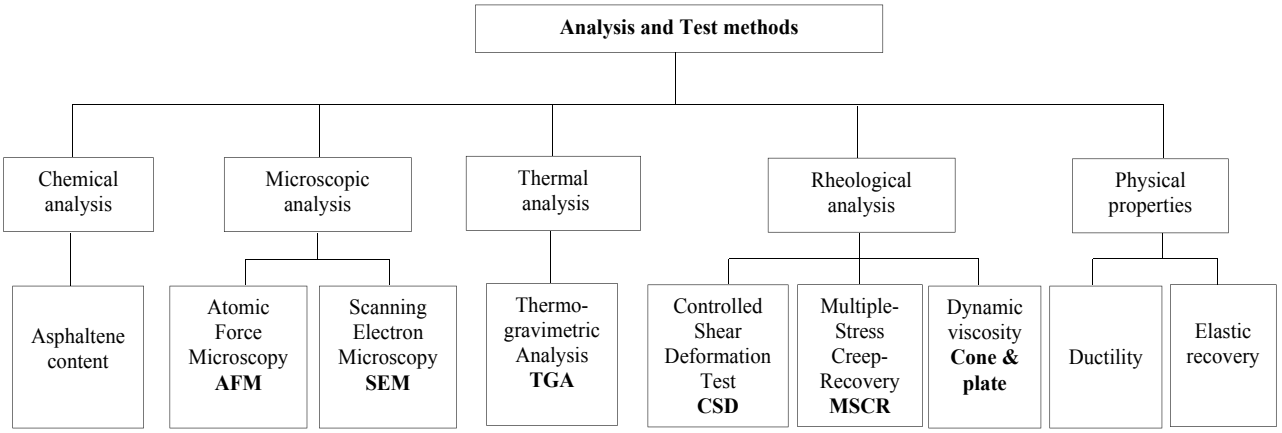

Fig. 2. Research plan.

Table 3
Asphaltene content of the bituminous binders

Description	Bitumen type		
	Paving-grade 70/100	Paving-grade 160/220	Industrial 160/220
Asphaltene content (%) (n-Heptane)	16.25	14.37	20.18
Asphaltene content (%) (n-Pentane)	23.16	21.6	N/A

4. Experimental works, results, and analysis

4.1. Chemical analysis; Asphaltene content

In the present research, a modified method based on ASTM D 6560 was applied for separating and quantifying the asphaltene content of the bitumens. For this purpose, in a vessel, a volume (in milliliters) of Chloroform ($CHCl_3$) was added to an amount (in grams) of bitumen (e.g., 3 g of bitumen for 3 mL of $CHCl_3$) and the mixture was then agitated carefully until the bitumen was dissolved. Then, a volume of n-Pentane and/or n-Heptane (forty times of the $CHCl_3$ volume) was added to the solution and was kept in darkness for a minimum of two hours while agitated occasionally. Finally, the precipitated asphaltenes were filtered, using a funnel with filter paper by vacuum (Whatman 42 ashless). It is worth mentioning that the test was carried out using both solvents (n-Pentane and n-Heptane). This was done because it was notified that the type of solvent has a significant effect on the tests' results. During the test, it was understood that n-Pentane was not a suitable solvent for industrial bitumen. This could be due to the difference between the asphaltene bonds or another dissoluble component in n-Pentan, which attests to the chemical difference between the bitumens. Table 3 represents the asphaltene content of the bitumens. According to the values, it can be seen that as expected, the 70/100 paving-grade showed the highest content of asphaltene while for the two softer bitumens the asphaltene contents were almost the same.

4.2. Microscopic analysis

4.2.1. Atomic Force Microscopy (AFM)

Introduced in 1986, the Atomic Force Microscope (AFM) has long been recognized as a useful tool for investigating the material's microstructure at micro and Nano-scale. AFM can be used to differentiate the bitumens based on their morphology [18]. Depending on the mode of measurement (Non-Contact Mode (NCM) or Pulsed-Force Mode (PFM)), either the surface topography or the mechanical properties of bitumen can be identified. In the AFM images of bitumen, four phases are typically observed: I) Catana phase consisting of topographic features also known as bee-structures; II) Peri phase consisting of the region surrounding the bee-structures; III) Para phase including the predominant smooth matrix; IV) Sal phase included high phase-contrast spots, very small and roughly circular [18, 19]. Accordingly, in the literature considering the aforementioned bitumen colloidal structure, the recognized phases via AFM could correspond to the four well-known chemical fractions of bitumen, SARA. However, it should be taken into account that until now there is no consensus

between the researchers on this claim. Considering the first hypothesis, the asphaltenes are referred to the bee structures (in some context also referred to the crystallized paraffin content of bitumen) [20]. The impression of "bees" stems from alternating higher and lower parts in the surface topography of it. Resins as the region surrounding the bee-structures so-called Peri phase, and aromatics and saturates as the smooth matrix, known as Para phase [13, 21–23]. However, as mentioned before, from the literature there is an evident gap between interpretations of the researchers.

In this research, the AFM samples were prepared by placing 20 ± 5 mg of bitumen on a steel plaque (12 mm diameter and 0.4 ± 0.08 mm thickness). The plaque was then kept at 100 ± 5 °C until the sample was melted, providing a smooth surface. Then the plaque was cooled to room temperature (~25 °C) with a cooling rate of 60 °C/h (fast cooling). It has been reported that the morphology of bitumen observed by means of AFM depends on the mode of conditioning (the rate of cooling the sample), evident in both phase contrast and topography images [24]. This phenomenon was also experienced here and observed by comparing the images obtained from differently-cooled samples.

Figure 3 shows the topography and phase images of the tested bitumen samples. The differences between the samples are quite evident. Comparing the two paving-grade bitumens, it can be seen that the 70/100 bitumen exhibited a rougher surface with larger bee structures in addition to an evident Para phase. From another perspective, comparing the paving-grade bitumens with the industrial one, the difference is more significant. While for the paving-grade 160/220 bitumen at least three main phases can be distinguished, for the industrial bitumen the Peri phase (attributed to resins) is more extended as the dominant phase. In addition, the bee structures were characterised with a flattened and diminished form for the industrial bitumen. The overall comparison implies the effect of Catana phase (bee structures) and Peri phase on the physical characteristics of the bitumens. Considering the bitumens' colloidal structure, it could be stated that the structure of the industrial bitumen is more similar to sol type bitumen with a more extended resin fraction, and the microstructure of the paving-grade bitumens are more similar to sol-gel type. The integrity of such analysis could be proven by the compatibility rate of these bitumens, where industrial bitumen showed high compatibility with high polymer content. Overall, according to the AFM images, the origin of the differences between the paving-grade and industrial bitumen relies on the chemical structure including asphaltene and malten phase characteristics, in particular, polar resins.

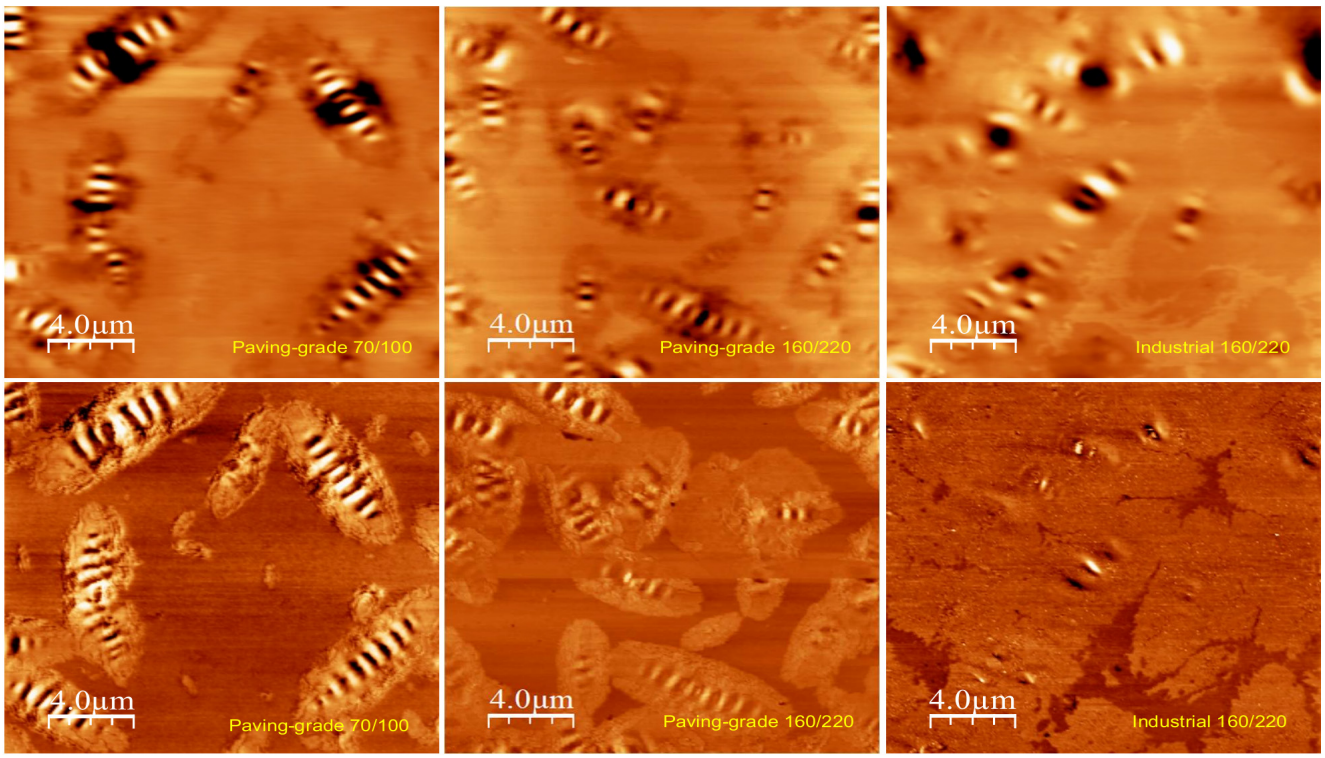

Fig. 3. AFM images. Phase images on the top and topography images in the bottom.

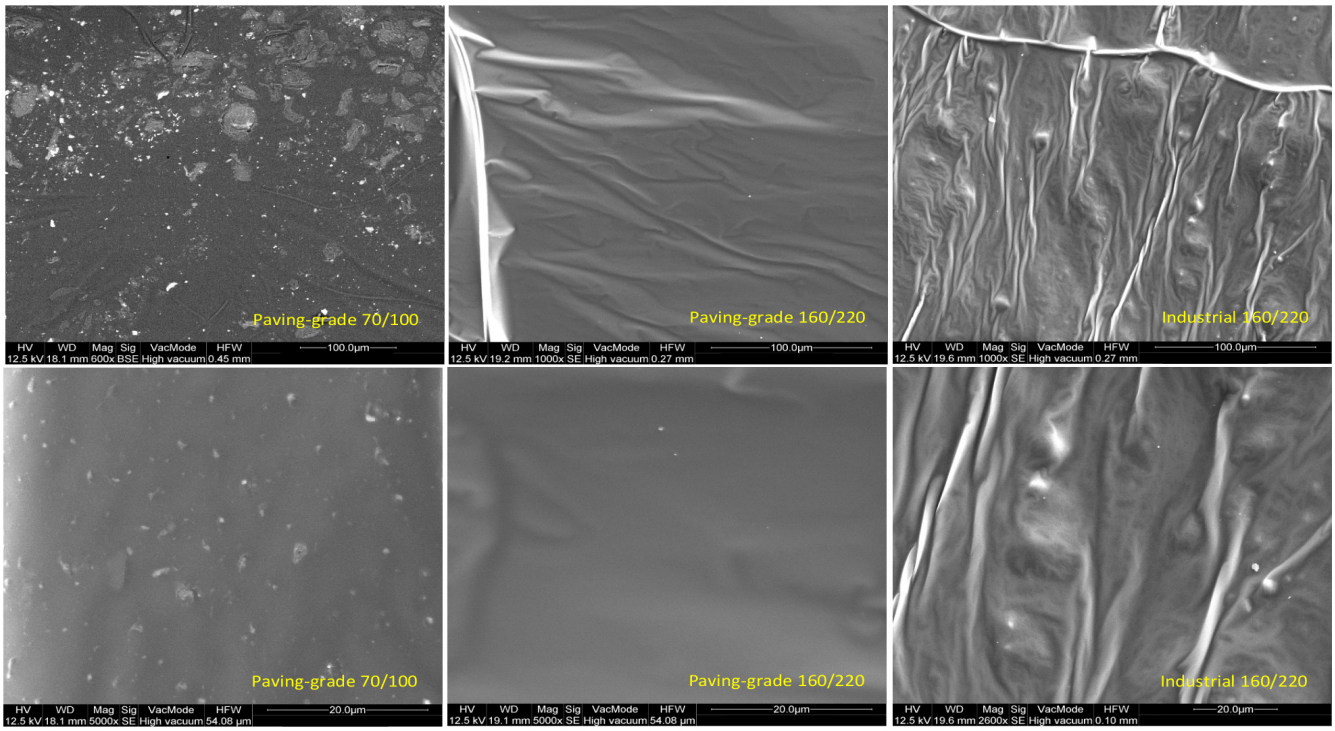

Fig. 4. SEM images at different magnitudes.

4.2.2. Scanning Electron Microscopy (SEM)

Another microscopic technique, which can provide insights into the structure of bitumen is the Scanning Electron Microscope (SEM) [25]. Whilst AFM and SEM have some significant differences, the observations are considered as complementary. Both devices involve interacting with a surface to generate an image; one using electrons and one using light. SEM also has a distinct advantage over AFM when it comes to determining the composition of a material [26]. However, the observation of bitumen structure with SEM is not easy. The high viscosity of bitumen at ambient temperature and its generally high-temperature sensitivity, its high oil content, and its colloidal behaviour make microscopic observation methods very difficult [27]. SEM generally does not permit observation of non-conducting oily samples because the resolution is too poor. Nevertheless, even if it does not allow observation of the oil phase, it still provides a very good resolution for the asphaltene skeleton, shown in several research works. The study of asphaltenes structure is useful to explain the bitumen rheological properties [28].

Figure 4 compares the SEM images of the tested bitumens at different magnitudes. As it can be seen, while the two paving-grade bitumens have a smooth surface, the industrial bitumen surface appears rough and with pores (somehow spongy). The obtained images get more significance when the surface of the bitumen by AFM is referred to the corresponding SEM images, showing a fundamental difference between industrial and paving-grade bitumens. Accordingly, for the industrial bitumen, the Peri phase (in AFM analysis) can be seen as a rough connected surface and the bee structures (high stiffness) as bright spots in some way covered by the so-called Peri phase within AFM. As for the paving-grade bitumens, the same relevance can be seen between the AFM and SEM images where the paving-grade 70/100 bitumen showed high-stiffness particles surrounded by limited and separated Peri phase.

4.3. Thermal Analysis; Thermogravimetric Analysis (TGA)

During its production, processing, and application, bitumen is always recognized as a temperature-dependent material. Thermal analysis for the characterization of bitumen is widely used today both in research and industry. Thermogravimetry (TG), or Thermo-Gravimetric Analysis (TGA), is a well-proved thermal analysing method for measuring the mass changes as a function of temperature or time [29]. In this research, the test was carried out on an approximately 3-mg sample of the bitumens and considering a heating rate of 10 °C/min in an air atmosphere. Figure 5 shows the TGA chromatograms of the bitumens, which were acquired from room temperature to 750 °C.

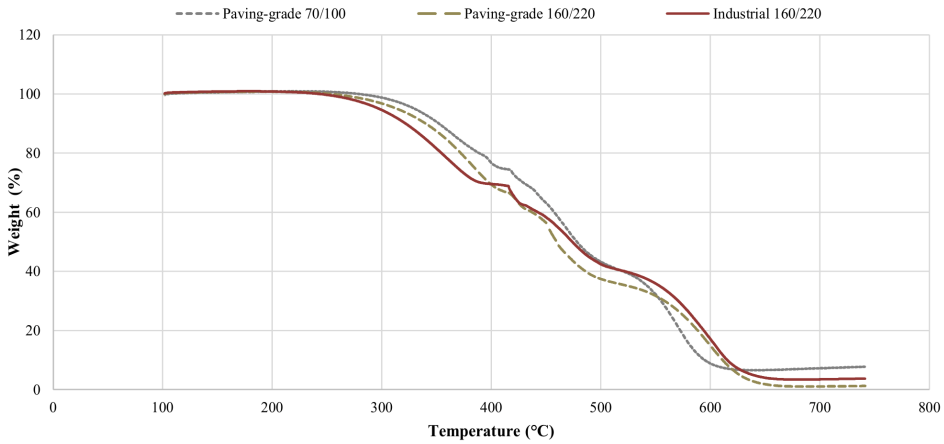

Fig. 5. Thermogravimetric analysis (TGA) of all investigated bitumens.

The chromatograms are characterized mainly by three distinct stages of the thermal decompositions of the bitumens. Accordingly, the first stage is characterized by continuous mass loss. This was observed due to the volatilization/reaction of low-boiling components, such as saturates and polar aromatics, which terminates at a temperature around 420 °C, regardless of the bitumen type. The second stage falls within the range of 420 to 510 °C (approximately), during which, the decomposition/volatilization of resins, along with aromatics and a few of the asphaltenes becomes highly prominent. It is noteworthy that as expected, the industrial bitumen showed a higher amount of resins compared to the same penetration paving-grade bitumen. Finally, the third stage is terminated at a high temperature of 610 °C for 70/100 paving-grade bitumen and 660 °C for the 2 soft bitumen binders. Therefore, the larger molecules decompose into smaller molecules in the gas phase. As shown in many chemical studies, the final remaining component of the bitumen sample is coke (i.e., generated by polymerization of asphaltene). Considering the final remaining, it can be declared that the 70/100 bitumen showed a higher quantity of asphaltenes compared to the softer bitumens, however, the industrial bitumen showed a higher content of the final remaining compared to the 160–220 paving-grade bitumen. In line with the other tests' results, this could be due to the higher Peri phase (probably resins as semi-rigid aromatics) of the industrial bitumen compared to the paving grade bitumens.

4.4. Rheological analysis

4.4.1. Rheological parameters

Given that the response of bitumen to stress is dependent on both temperature and loading time, the rheology of bitumen is defined by its stress-strain-time-temperature response [30]. The rheological properties of bitumen are generally expressed in terms of complex modulus (G*), phase angle (δ), and complex viscosity (η*). The complex modulus is considered as the stiffness parameter of a binder that includes its viscos and elastic properties and the phase angle is generally used to separate the viscosity from the elastic components [31–34]. Materials that behave like elastic solid have a low phase angle. The more a bitumen behaves like a fluid, the higher the phase angle would be.

The rheological analysis, using DSR, generally starts with the amplitude sweep test. It determines the linear viscoelastic range and its limits. A typical measurement profile for an amplitude sweep is a logarithmic increase of the strain from 0.01% to 100% with five measuring points per decade and a constant angular frequency (ω) of 10 rad/s. A diagram of such settings for the tested bitumens is given in Fig. 6. The tests have been done at 10 °C using 8 mm plate-plate geometry. The data for LVE range is then used for the following frequency sweep tests. According to the obtained profiles, it can be seen that apart from the origin of the bitumens, the level of penetration has a great effect on the linear LVE range. While the two 160/220 bitumen showed similar behaviour and the profile of the 70/100 bitumen is evidently different.

Having the LVE of the bitumens, the dynamic visco-elastic parameters of materials were determined adopting Controlled Shear Deformation test (CSD) - Frequency Sweep (FS) under the following test conditions:

- temperatures: 0–90 °C, with 10-degree steps;
- frequencies: 0.01–10 Hz (nineteen values);

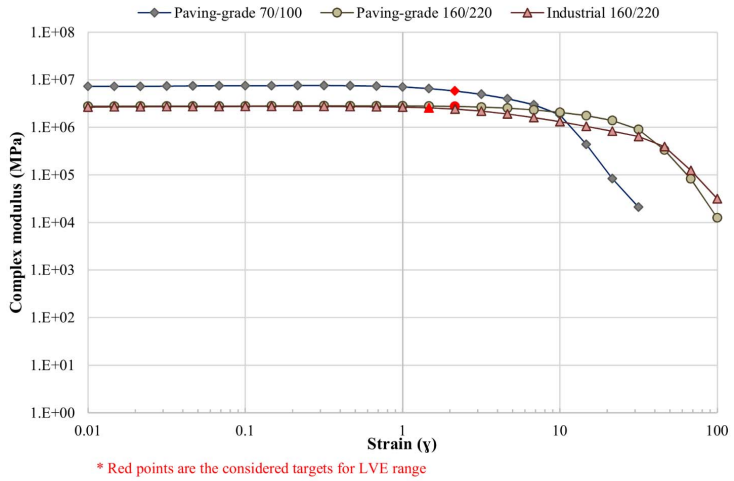

Fig. 6. Amplitude sweep diagrams at 10 °C.

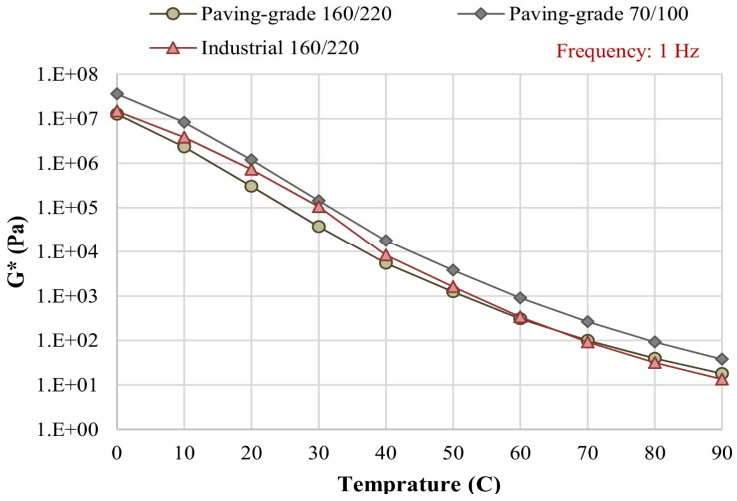

Fig. 7. Compared isochronal plots of the complex shear moduli.

• parallel plate geometries: 8 mm diameter with a 2 mm gap (low to intermediate temperatures; 0–30 °C); 25 mm diameter with a 1 mm gap (high temperatures 40–90 °C);

• strain amplitude: within LVE response according to the value obtained from AS test.

The DSR rheological data for the bitumens were then presented in the form of isochronal plots of complex modulus and phase angle at a reference frequency of 1 Hz. In addition, for providing complete data for the analysis, the black diagrams of the tested bitumens were compared.

G* is defined as the ratio of maximum (shear) stress to maximum strain and provides a measure of the total resistance to deformation when the bitumen is subjected to shear loading. Superpave considers the complex modulus as the stiffness of the bitumen including its elastic properties. The G* isochronal plot for the tested bitumens at 1 Hz is shown in Fig. 7. Accordingly, it can be seen that the 160/220 paving-grade bitumen showed a lower G* compared to the industrial bitumen in the tested temperature range up to approximately 50 °C, from which the difference is insignificant. This could be due to the presence of high paraffinic constituent content of industrial bitumen, which was previously seen by AFM images. Through the low to medium level of temperatures, the contradiction of the paraffinic constituents makes bitumen harder and at higher temperatures acts in contrary, compared with the same penetration grade paving bitumen. From another perspective, comparing the types of bitumen, as it could be expected throughout all the test temperature range, the 70/100 bitumen is stiffer than both 160/220 bitumens.

In rheological tests with the DSR, the phase angle is an indirect measure of how fluid the material is. The more a material behaves like a fluid, the higher the phase angle. Materials that behave like elastic solid have a lower phase angle [35].

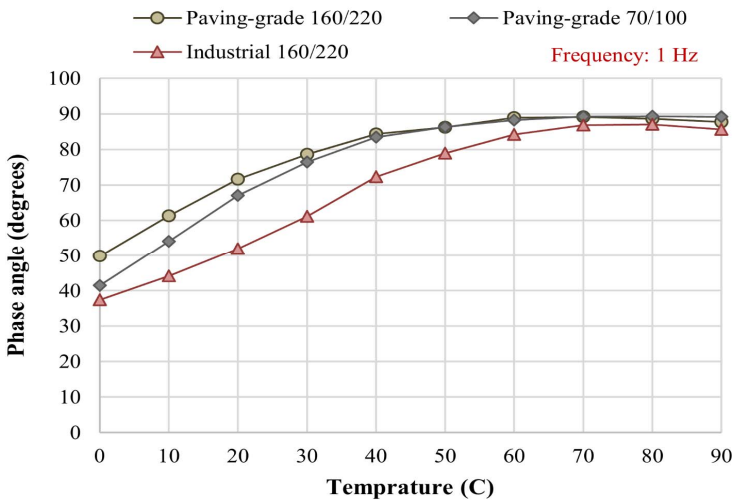

Fig. 8. Compared isochronal plots of the phase angle.

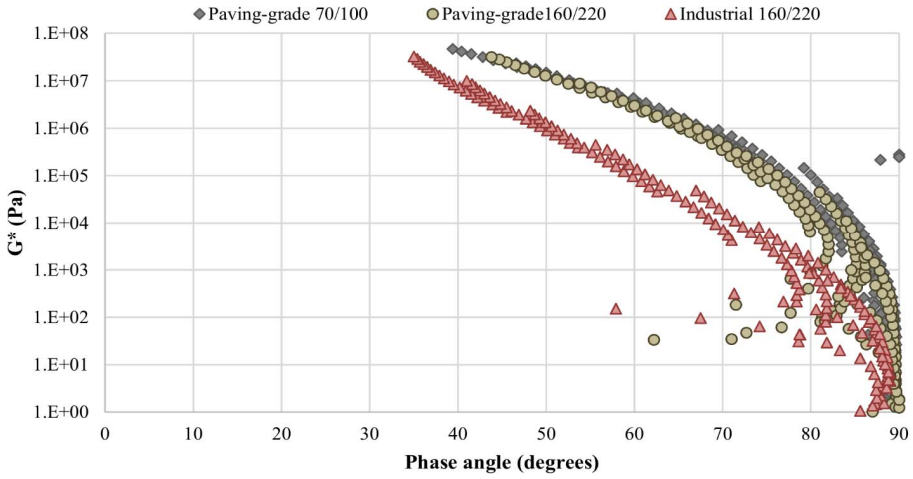

Fig. 9. Black diagrams.

The phase angle is a measure of the viscoelastic balance of bitumen behaviour as tan δ = G”/G’, where G’ is the storage modulus and G” is the loss modulus of the material [36]. According to the results shown in Fig. 8, it can be seen that while both of the paving-grade bitumens showed the same viscoelastic response especially after 40 °C, the industrial bitumen showed a greater elastic response compared to paving-grade ones.

Besides the isochronal plots, *Black diagrams* were also drawn to analyse the obtained rheological data from another perspective. As *Black diagrams* do not require any manipulation of the rheological data before data representation, they provide a quick and suitable means of identifying differences in rheological data and the breakdown of time-temperature equivalence and thermo-rheological simplicity [37]. According to Fig. 9, it can be seen that the *Black diagram* allows the unique rheological characteristics of the industrial bitumen to be identified. Compared to the paving-grade bitumens, the industrial bitumen showed the presence of an elastic constituent differently compared to those paving-grade ones. A shifting of the rheological data more towards a lower phase angle (greater elastic behaviour) depicts this. However, compared to the typical black diagrams of SBS, EVA, etc. it differs. While for such those PmBs, the plots tend to lower phase angle at higher temperatures, making a curve plateau, here with decreasing the G*, the phase angles get more close. This behaviour is also can be seen in the isochronal plots where, at higher temperatures the behaviour of bitumens were similar, and at medium to low temperatures, the industrial bitumen showed higher stiffness.

4.4.2. Elastic response

Multiple Stress Creep Recovery (MSCR) test is the latest improvement to the Superpave

Table 4
Non-recoverable compliance and recoverable strain 46 °C

Bitumen	Non-recoverable compliance-Jnr (1/kPa)		Recoverable strain-R (%)	
	0.1 (kPa)	3.2 (kPa)	0.1 (kPa)	3.2 (kPa)
Paving-grade 70/100	0.597	0.627	7.62	3.39
Paving-grade 160/220	1.466	2.202	19.09	1.57
Industrial 160/220	1.963	2.327	5.82	0.08

Performance Grade (PG) specifications and a reliable alternative to the G*/sin δ parameter. The test uses a well-established creep and recovery concept to evaluate the binder's potential for permanent deformation. It was also introduced to evaluate bituminous materials at high service temperatures, in particular, to evaluate the stress or loading resistance [38]. A single MSCR test can provide information on both the performance and level of modification of the bitumen [39]. In the MSCR test, using DSR, a 1-second creep load is applied to a bitumen sample. After the 1-second, the load is removed and the sample is allowed to recover for 9 sec. The test is started with the application of low stress (0.1 kPa) for 10 creep/recovery cycles then the stress increased to 3.2 kPa and repeated for an additional 10 cycles. The MSCR test measures the non-recoverable creep compliance (Jnr) and percent recovery (R). Jnr (compliance) is inversely related to the complex modulus. The lower the Jnr value the stiffer the bitumen. Percent recovery shows how readily the sample will return to its original shape after being subjected to a load or stress.

According to the results shown in Table 4, the paving-grade 160–220 bitumens showed considerably larger elastic properties compared to the Industrial bitumen of the same pen grade. For the paving-grade 70/100 bitumen, as it could be expected the recoverable strain at 0.1 kPa was less compared with the paving-grade bitumen 160/220 and vice versa at 3.2 kPa. This could be due to the chemical structure of this bitumen with a higher content of asphaltene as stiffness at higher temperatures, which has been shown in the upper section.

4.4.3. Viscosity

The viscosity of bitumen is its internal resistance to flow or measure of its resistance to deformation by either shear stress or tensile stress. Bitumen viscosity is one of the most important processing and service properties. There are various definitions of viscosity and several testing methods to measure it. In practice, it influences the workability and resistance to mix both in pavement construction and other industrial applications [40]. For the present research, the dynamic viscosity of the bitumens was tested using DSR, applying cone and plate method (50 mm diameter was used) according to EN 13702. The test involves the determination of torque for a pre-set shear rate. Using a known torque and cone factor, the testing system calculates the viscosity based on the following equation:

$$\eta = \frac{A \cdot Md}{\gamma}$$

where: A is the cone factor expressed m^{-3}; Md is the torque expressed in N.m; and γ is the shear rate expressed in s^{-1}.

Figure 10 represents the dynamic viscosity of the tested bitumens at two different temperatures. According to the results it can be seen that while the dynamic viscosity of 70/100 bitumen is significantly higher compared to 160/220 bitumens, the difference between the paving-grade and industrial bitumens is not that much. This implies that from a viscosity point of view at high temperatures, the 160/220 bitumens act similarly as has been shown within isochronal plots and the balk diagram.

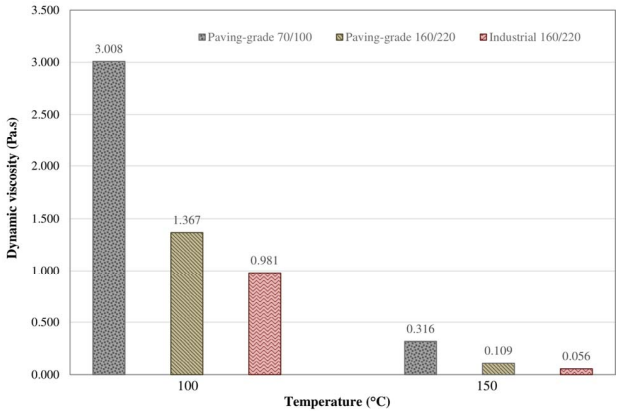

Fig. 10. Dynamic viscosity of Industrial bitumen vs. paving-grade bitumens.

Table 5
Ductility and elastic recovery

Description	Standard	Bitumen type		
		Paving-grade 70/100	Paving-grade 160/220	Industrial 160/220
Ductility (mm)	ASTM D 113	113	143	112
Elastic recovery (%)	EN 13398	10	21	15

4.5. Ductility and conventional Elastic recovery

The ductility of bitumen is its property to elongate under traffic load without getting cracked in road pavement construction works. Hence, it is assumed that it makes the pavement more resistant to cracks [41]. As ASTM D 113, the ductility of a bituminous material is measured by the distance to which it will elongate before breaking when two ends of a piece of the material (in a special form), are pulled apart at a specified speed and a specified temperature.

The elastic recovery of bitumen is considered as an indication of bitumen's cohesion and potential self-healing properties. Within conventional testing methods, the test involves the determination of bitumen elasticity being the distance between the ends of a stretched and cut sample under pre-set conditions. Here, the elastic recovery of the bitumens was determined using a ductilometer according to EN 13398. The standard is especially applicable to bituminous binders modified with thermoplastic elastomers, but it can be also used with other bituminous binders, which generate only limited recovery.

The ductility and elastic recovery tests were conducted using at least three repetitions providing an understanding of the differences between the ductility and elastic properties of the industrial and paving-grade bitumens. The test results are shown in Table 5. According to the values, the paving-grade 160/220 showed the highest ductility and elastic recovery. Notably, the same behaviour was observed via MSCR test results. As it could be expected the paving-grade 70/100 bitumen showed lower ductility and recovery compared to that of 160/220, which could be due to the high amount of asphaltene.

5. Conclusions

The main objective of this study was to investigate the differences between industrial bitumens (not the oxidized ones) and paving-grade bitumens. For this purpose, an interdisciplinary approach was implemented and a wide range of tests was carried out, providing comprehensive and detailed knowledge. The follows are some of the main concluding remarks:

- Asphaltene separation showed that there is a significant difference not only between the asphaltene content but also the whole chemical structure of the tested bitumen. Not the same solvent wasapplicable for asphaltene separation of the bitumens.

- The comparison of the AFM images showed this method as an efficient approach in bitumen micro-structural investigations. Apart from what the bee structures refer to, both topography and phase images exhibited more concentration of bee structures for the paving-grade bitumens with bigger in size and rougher surface compared to the industrial bitumen with the same penetration. In addition, for the industrial bitumen, the Peri phase (in some references attributed to the resins) was the domain phase, observed.

- Stress/loading behaviour of the paving-grade and industrial bitumen in terms of non-recoverable creep compliance (Jnr) and percent recovery (R) was compared by MSCR test. According to the results, the paving-grade bitumen 160/220 showed the highest elastic recovery among the tested bitumens. This was in line with the conventional elastic recovery and ductility tests' results.

- The dynamic viscosity of the bitumens was determined by means of DSR using cone and plate set up at 2 different temperatures. The lowest viscosity was always recorded for the industrial bitumen, which could be related to the saturate/wax content and asphaltene characteristics observed via microscopic images. The results were in line with the other rheological data and the bitumen aspects, where the industrial bitumen showed paste-like (toothpaste) material at medium to high levels of temperatures.

Acknowledgment

The authors would like to acknowledge the contribution of the R&D department of POLYGLASS S.p.A. for providing some of the tested materials.

References

[1]. The bitumen industry: a global perspective: production, chemistry, use, specification and occupational exposure, 3rd ed., Asphalt Institute Inc. and European Bitumen Association – Eurobitume, 2015. ISBN: 9781934154731

[2]. The asphalt paving industry: a global perspective, 3rd ed., National Asphalt Pavement Association and European Asphalt Pavement Association. 2011. ISBN 0-914313-06-1.

[3]. The bitumen roofing industry – a global perspective: production, use, properties, specifications and occupational exposure, 2nd ed., The Asphalt Roofing Manufacturers Association, The Bitumen Waterproofing Association, The National Roofing Contractors Association, The Roof Coatings Manufacturers Association, 2011. ISBN 978-0-9815948-3-5

[4]. Oxidized Bitumen, Raha Bitumen Company, available online 27/03/2020 at: http://rahabitumen.com/oxidized-bitumen/

[5]. Road paving bitumen, Alma Petroli, available online 27/03/2020 at: https://www.almapetroli.com/en/road-paving-bitumen

[6]. C. Oliviero Rossi, P. Caputo, S. Ashimova, A. Fabozzi, G. D'Errico, R. Angelico, *Appl. Sci.* 8 (2018) 1405. DOI: 10.3390/app8081405

[7]. Y. Becker, M.P. Méndez, Y. Rodríguez, Polymer modified asphalt. Vision Tecnologica 9 (2001) 39–50.

[8]. P. Caputo, M. Porto, V. Loise, B. Teltayev, C. Oliviero Rossi, *Eurasian Chem.- Technol. J.* 21, (2019) 235–239. DOI: 10.18321/ectj864

[9]. Bitumen 160/220 for industrial uses, https://oilproducts.eni.com/en_GB/, 2017 (Accessed 18 March 2020).

[10]. N. Nciri, N. Kim, N. Cho, *Mater. Chem. Phys.* 193 (2017) 477–495. DOI: 10.1016/j.matchemphys.2017.03.014

[11]. C. Giavarini, P. De Filippis, M.L. Santarelli, M. Scarsella, *Fuel* 75 (1996) 681–686. DOI: 10.1016/0016-2361(95)00312-6

[12]. J. Read, D. Whiteoak, R. Hunter, Robert Hunter, The Shell Bitumen Handbook. Thomas Telford Publishing; 5th edition, 2003. ISBN-10: 072773220X

[13]. D. Lesueur, *Adv. Colloid Interfac.* 145 (2009) 42–82. DOI: 10.1016/j.cis.2008.08.011

[14]. H. Zhang, Building Materials in Civil Engineering. Woodhead Publishing Series in Civil and Structural Engineering 423 (2011) 253–288. DOI: 10.1533/9781845699567.253

[15]. C. Oliviero Rossi, P. Caputo, G. De Luca, L. Maiuolo, S. Eskandarsefat, C. Sangiorgi, *Appl Sci.* 8 (2018) 229. DOI: 10.3390/app8020229

[16]. C. Oliviero Rossi, P. Caputo, V. Loise, S. Ashimova, B. Teltayev, C. Sangiorgi, (2019) A New Green Rejuvenator: Evaluation of Structural Changes of Aged and Recycled Bitumens by Means of Rheology and NMR. In: Poulikakos L., Cannone Falchetto A., Wistuba M., Hofko B., Porot L., Di Benedetto H. (eds) RILEM 252-CMB Symposium. RILEM 252-CMB 2018. RILEM Bookseries, vol 20. Springer, Cham. DOI: 10.1007/978-3-030-00476-7_28

[17]. P. Caputo, V. Loise, S. Ashimova, B. Teltayev, R. Vaiana, C. Oliviero Rossi, *Colloid. Surface. A* 574 (2019) 154–161. DOI: 10.1016/j.colsurfa.2019.04.080

[18]. J-F. Masson, V. Leblond, J. Margeson, *J. Microsc.* 221 (2006) 17–29. DOI: 10.1111/j.1365-2818.2006.01540.x

[19]. A.T. Pauli, J.F. Branthaver, R.E. Robertson, W. Grimes, C.M. Eggleston. Heavy Oil and Resid Compatibility and Stability. San Diego, Calif, USA: Division of Petroleum Chemistry, American Chemical Society; 2001. Atomic force microscopy investigation of SHRP asphalts; pp. 110–114.

[20]. P. Calandra, P. Caputo, M.P. De Santo, L. Todaro, V. Turco Liveri, C. Oliviero Rossi, *Constr. Build. Mater.* 199 (2019) 288–297. DOI: 10.1016/j.conbuildmat.2018.11.277

[21]. A.L. Lyne, V. Wallqvist, B. Birgisson, *Fuel* 113 (2013) 248–256. DOI: 10.1016/j.fuel.2013.05.042

[22]. L. Loeber, O. Sutton, J. Morel, J.-M. Valleton, G. Muller, *J. Microsc*. 182 (1996) 32–39. DOI: 10.1046/j.1365-2818.1996.134416.x

[23]. A. Jager, R. Lackner, C. Eisenmenger-Sittner, R. Blab, *PAMM* 4 (2004) 400–401. DOI: 10.1002/pamm.200410181

[24]. A.T. Pauli, R.W. Grimes, A.G. Beemer, T.F. Turner, J.F. Branthaver, *Int. J. Pavement Eng.* 12 (2011) 291–309. DOI: 10.1080/10298436.2011.575942

[25]. P. Mikhailenko, H. Kadhim, H. Baaj, S. Tighe, *J. Microsc.* 267 (2017) 347–355. DOI: 10.1111/jmi.12574

[26]. The Differences Between Atomic Force Microscopy and Scanning Electron Microscopy, AZO MATERIALS, https://www.azom.com/article.aspx?ArticleID=11879, 2015 (Accessed 18 April 2020).

[27]. L. Loeber, J. Morel, O. Sutton, J.-M. Valleton, G. Muller, *Atomic Force Microscopy/Scanning Tunneling Microscopy* 3 (1999) 205–208. DOI: 10.1007/0-306-47095-0_20

[28]. K. Pospíšil, A. Frýbort, A. Kratochvíl, J. Macháčková, *Trans. Transp. Sci*. 1 (2008) 13–20. DOI: 10.5507/tots.2008.002

[29]. P. Caputo, G.A. Ranieri, N. Godbert, I. Aiello, A. Tagarelli, C. Oliviero Rossi, *Med. J. Chem.* 7

(2018) 259–266. DOI: 10.13171/mjc74181107-rossi
[30]. G.D. Airey, *Int. J. Pavement Eng*. 5 (2004) 137–151. DOI: 10.1080/10298430412331314146
[31]. V.O. Bulatovic, V. Rek, J. Markovic, *Polym. Eng. Sci.* 54 (2014) 1056–1065. DOI: 10.1002/pen.23649
[32]. M. Porto, P. Caputo, V. Loise, G. De Filpo, C. Oliviero Rossi, P. Calandra, *Appl. Sci.* 9 (2019) 5564. DOI: 10.3390/app9245564
[33]. C. Oliviero Rossi, P. Caputo, V. Loise, D. Miriello, B. Teltayev, R. Angelico, *Colloid. Surface. A* 532 (2017) 618–624. DOI: 10.1016/j.colsurfa.2017.01.025
[34]. M. Porto, P. Caputo, V. Loise, S. Eskandarsefat, B. Teltayev, C. Oliviero Rossi, *Appl. Sci.* 9 (2019) 742. DOI: 10.3390/app9040742
[35]. National Academies of Sciences, Engineering, and Medicine. 2011. Special Mixture Design Considerations and Methods for Warm-Mix Asphalt: A Supplement to NCHRP Report 673: A Manual for Design of Hot-Mix Asphalt with Commentary. Washington, DC: The National Academies Press. DOI: 10.17226/14615
[36]. G.D. Airey, *J. Mater. Sci*. 39 (2004) 951–959. DOI: 10.1023/B:JMSC.0000012927.00747.83
[37]. G.D. Airey, *Road Mater. Pavement* 3 (2002) 403–424. DOI: 10.1080/14680629.2002.9689933
[38]. H. Soenen, T. Blomberg, T. Pellinen, O. Laukkanen, *Road Mater. Pavement* 14 (2013) 2–11. DOI: 10.1080/14680629.2013.774742
[39]. The multiple stress creep recovery (MSCR) procedure. TechBrief, Federal Highway Administration, FHWA-HIF-11-038, April 2011.
[40]. S. Arafat Yero, M.Rosli Hainin, *ARPN Journal of Science and Technology* 2 (2012) 422–426.
[41]. G.A.J. Mturi, M. Nkgapele, Force ductility – a 5 year feedback of performance results. Abstracts of the 32nd Southern African Transport Conference, 8–11 July 2013, Pretoria, South Africa. ISBN 978-1-920017-62-0